Validation of chemical compound library screening for transcriptional co-activator with PDZ-binding motif inhibitors using GFP-fused transcriptional co-activator with PDZ-binding motif

Shunta Nagashima,[1] Junichi Maruyama,[1] Shodai Kawano,[1] Hiroaki Iwasa,[1] Kentaro Nakagawa,[1] Mari Ishigami-Yuasa,[2] Hiroyuki Kagechika,[2,3] Hiroshi Nishina[4] and Yutaka Hata[1,5]

[1]Department of Medical Biochemistry, Graduate School of Medical and Dental Sciences, Tokyo Medical and Dental University, Tokyo; [2]Chemical Biology Screening Center, Tokyo Medical and Dental University, Tokyo; [3]Institute of Biomaterials and Bioengineering, Tokyo Medical and Dental University, Tokyo; [4]Department of Developmental and Regenerative Biology, Medical Research Institute, Tokyo Medical and Dental University, Tokyo; [5]Center for Brain Integration Research, Tokyo Medical and Dental University, Tokyo, Japan

Transcriptional co-activator with PDZ-binding motif (TAZ) plays versatile roles in cell proliferation and differentiation. It is phosphorylated by large tumor suppressor kinases, the core kinases of the tumor-suppressive Hippo pathway. Phosphorylation induces the cytoplasmic accumulation of TAZ and its degradation. In human cancers, the deregulation of the Hippo pathway and gene amplification enhance TAZ activity. TAZ interacts with TEA domain family members (TEAD), and upregulates genes implicated in epithelial–mesenchymal transition. It also confers stemness to cancer cells. Thus, TAZ activation provides cancer cells with malignant properties and worsens the clinical prognosis. Therefore, TAZ attracts attention as a therapeutic target in cancer therapy. We applied 18 606 small chemical compounds to human osteosarcoma U2OS cells expressing GFP-fused TAZ (GFP-TAZ), monitored the subcellular localization of GFP-TAZ, and selected 33 compounds that shifted GFP-TAZ to the cytoplasm. Unexpectedly, only a limited number of compounds suppressed TAZ-mediated enhancement of TEAD-responsive reporter activity. Moreover, the compounds that weakened TEAD reporter activity did not necessarily decrease the unphosphorylated TAZ. In this study, we focused on three compounds that decreased both TEAD reporter activity and unphosphorylated TAZ, and treated several human cancer cells with these compounds. One compound did not show a remarkable effect, whereas the other two compounds compromised the cell viability in certain cancer cells. In conclusion, the GFP-TAZ-based assay can be used as the first screening for compounds that inhibit TAZ and show anticancer properties. To develop anticancer drugs, we need additional assays to select the compounds.

Transcriptional co-activator with PDZ-binding motif (TAZ, also called WWTR1) was discovered as a molecule that interacts with 14-3-3 and was later identified to be a target of the tumor-suppressive Hippo pathway.[1,2] TAZ has the TEA domain family member (TEAD)-binding region in the N-terminus, the WW domain in the middle region, and the DNA activation domain in the C-terminus.[3] TAZ is phosphorylated at four serine residues by large tumor suppressor kinases (LATS1/2), which are the core kinases of the Hippo pathway.[4] The phosphorylation at serine 89 generates the 14-3-3-binding motif, so that 14-3-3 traps the phosphorylated TAZ in the cytoplasm.[3] The phosphorylation at serine 66 or 311 triggers the degradation of TAZ.[5,6] That is, the Hippo pathway negatively regulates TAZ and suppresses the TAZ-dependent gene transcription. In human cancers, the deregulation of the Hippo pathway and *TAZ* gene amplification result in the high activation of TAZ.[7] TAZ upregulates the genes that are implicated in epithelial–mesenchymal transition and drug resistance[4] and confers stemness to cancer cells.[8] TAZ also

cross-talks with the Wnt pathway. The cytoplasmic TAZ blocks the phosphorylation by casein kinases of Disheveled, binds β-catenin, and promotes β-catenin degradation.[9–11] It follows that the deregulation of the Hippo pathway increases the nuclear β-catenin and augments the Wnt signaling. Through these mechanisms, the hyperactive TAZ increases the incidence of metastasis and recurrence. The clinical data demonstrate that TAZ expression correlates with short survival of patients with cancers.[12,13] We can expect to improve the prognosis by the inhibition of TAZ, especially in cancers with the compromised Hippo pathway.

Yes-associated protein 1 (YAP1) is the paralogue of TAZ.[1,2] It is also phosphorylated by LATS kinases and the phosphorylation induces the translocation of YAP1 into the cytoplasm and the degradation. YAP1 co-operates with TEAD and its activation is associated with poor clinical prognosis in cancers.[14–17] We expressed GFP-YAP1 in human osteosarcoma U2OS cells and evaluated the localization of GFP-YAP1 under various conditions.[18] When the cells are confluent, GFP-YAP1 is mainly

detected in the cytoplasm but when the cells are sparse, GFP-YAP1 is accumulated in the nucleus. This observation suggests that the Hippo pathway, as the sensor of cell density, is intact in U2OS cells. To identify the compounds that affect the Hippo pathway, we treated the cells with several compounds for 4 h, and revealed that dobutamine decreases the unphosphorylated nuclear GFP-YAP1.[18] We confirmed that dobutamine inhibits YAP1 through β-adrenergic receptor. In response to our report, Fujii discussed the possibility of dobutamine as a YAP1-targeted anticancer drug and it was echoed by the report that dobutamine inhibits human gastric cancer.[19,20]

In this study, we used U2OS cells expressing GFP-TAZ to search the compounds that inhibit TAZ through the Hippo pathway. We tested 18 606 small chemical compounds and treated the cells with the compounds for 24 h. Despite the above-mentioned report about the effect of dobutamine on gastric cancer, we could not detect a significant effect of dobutamine on cancer cells (data not shown). This is the reason why we treated the cells with the compounds for a longer time, expecting to obtain compounds with a longer inhibitory effect. We obtained 33 compounds that increased the ratio of the cytoplasmic GFP-TAZ over the nuclear GFP-TAZ. We characterized these compounds. We aimed here to answer two questions: Can we obtain, by use of this cell-based assay, the compounds that inhibit TAZ through the Hippo pathway? If we obtain such compounds, do they show an inhibitory effect against cancer cells? In this work, we report two compounds that increase the cytoplasmic TAZ. These compounds decrease the unphosphorylated TAZ and suppress the viability in several human cancer cells. Through the characterization of these two compounds, we discuss the validity and the limitation of this cell-based assay.

Materials and Methods

DNA constructions and virus production. pCIneoFLAG, pCIneoFLAG-His6 (pCIneoFH), pCIneoFLAG-His6-FLAG (pCIneoFHF), pCIneoMyc, pCIneoEGFPC2, pCIneoLuc, pLL3.7-EGFPC2-TAZ, pLL3.7-FLAG-YAP1, pCIneoFH-TAZ, pFLAG-YAP1, pCIneoLuc-TAZ, pCIneoFH-TAZ S89A, pCIneoFLAG-LATS1, pCIneoLuc-protein phosphatase (PP)1A, and pCIneoLuc-PP2A were described previously.[18,21–24] pCIneoFHF-PP1A and pCIneoFHF-PP2A were prepared by ligating *Eco*RI/*Sal*I fragments from pCIneoLuc-PP1A and pCIneoLuc-PP2A into pCIneoFHF. pCIneoEGFPC2-TAZ S89A was prepared by ligating the *Eco*RI/*Not*I fragment from pCIneoFH-TAZ S89A into pCIneoEGFPC2. pCIneoFLAG-LATS1 was generated by ligating *Mlu*I/*Sal*I fragments from pCIneoMyc-LATS1 into pCIneoFLAG. The *Nhe*I/*Eco*RI fragment from pLL3.7-FLAG-YAP1 was ligated into pCIneo (Promega, Madison, WI, USA) to generate pCIneoFLAG2. The *Eco*RI/*Dra*I fragment from pEGFPN3 (Clontech, Moutain View, CA, USA) was ligated into *Eco*RI/*Sma*I sites of pCIneoFLAG2 vector to generate pCIneoFLAG-GFP. 8xGT-IIC-δ51LucII luciferase reporter, pcDNA-LATS2-FLAG, and pCMV alkaline phosphatase were gifts from Hiroshi Sasaki, Tadashi Yamamoto, and Sumiko Watanabe, respectively.[25,26] Lentivirus was generated by using HEK293 cells as packaging cells.

Antibodies and reagents. The antibodies and the reagents were obtained from commercial sources: mouse anti-GFP (SC-9996; Santa Cruz Biotechnology, Dallas, TX, USA); Hoechst 33342 and mouse β-actin (A1978; Sigma-Aldrich, St. Louis, MO, USA); anti-DYKDDDDK-tag (014-22383), anti-DYKDDDDK-tag beads (016-22784), and Phos-tag acrylamide (Wako Pure Chemical Industries, Osaka, Japan); and rabbit

anti-S909/S871 LATS1/2 (#9157S) and rabbit anti-YAP/TAZ (D24E4) (#8418) (Cell Signaling Technology, Danvers, MA, USA). Rabbit anti-phospho-S89 TAZ and anti-T1079/T1041 LATS1/2 antibodies were described previously.[23,27]

Cell cultures, gene introduction, and screening. HEK293, U2OS, H1299, SW480, and U87MG cells were cultured in DMEM containing 10% (v/v) FBS and 10 mM HEPES–NaOH (pH 7.4) under 5% CO_2 at 37°C. OVCAR5 and U373 cells were cultured in RPMI-1640 containing 10% (v/v) FBS and 10 mM HEPES–NaOH (pH 7.4) under 5% CO_2 at 37°C. DNA transfection was carried out with Lipofectamine 2000 (Thermo Fisher Scientific, Waltham, MA, USA). U2OS cells expressing GFP-TAZ were established by using pLL3.7 EGFPC2-TAZ lentivirus vector. The nucleus was visualized with Hoechst 33342 and the GFP signals inside and outside the nucleus were measured by ArrayScan VTI (Thermo Fisher Scientific, Waltham, MA, USA). We obtained the ratio of the inside signal over the outside signal as the nucleus/cytoplasm (n/c) ratio. In the first screening, 80 compounds were assayed in one 96-well plate with a control. Due to the small number of samples in one plate, to minimize the effect of outliers, we calculated robust Z-scores (Robust Z-score = $|x -$ median $(x)|$ / normalized interquartile range) by use of Microsoft Excel (Microsoft, Redmond, WA, USA).

Quantitative RT-PCR. Quantitative RT-PCR analysis was carried out by using SYBR Green (Roche, Penzberg, Germany) and ABI7500 Real-Time PCR system (Thermo Fisher Scientific, Waltham, MA, USA). The primers were: human GAPDH, 5′-ccactcctccacctttgac-3′ and 5′-accctgttgctgtagcca-3′; human connective tissue growth factor, 5′-ccaatgacaacgcctcctg-3′ and 5′-tggtgcagccagaaagctc-3′; and human Cyr61, 5′-agcctcgcatcctatacaacc-3′ and 5′-ttctttcacaaggcggcactc-3′.

RNA interference. RNA interferences were carried out with Lipofectamine RNAiMAX (Thermo Fisher Scientific). The double-stranded RNAs were purchased from Thermo Fisher Scientific: s17392 for human LATS1, s25505 for human LATS2, s24789 for human TAZ, s20366 for human YAP1, and Silencer Select negative control No. 2 #4390846. The validity of the knockdown was confirmed by quantitative RT-PCR or immunoblotting.

Reporter assay. HEK293 cells (8×10^5) were plated in one well of a collagen-coated 6-well plate. The cells were transfected with 0.3 μg 8xGT-IIC-δ51LucII luciferase reporter, 0.3 μg pCMV alkaline phosphatase, and 0.012 μg pCIneoFH-TAZ or pFLAG-YAP1. Eighteen hours later, the cells from one well were replated into 11 wells of a 24-well plate, treated with 10 μM each compound for 24 h, and harvested. The cells were lysed in 100 μL lysis buffer (25 mM Tris-HCl [pH 7.4], 2 mM DTT, 2 mM EDTA, 4 mM EGTA, 4 mM $MgCl_2$, 1% [v/v] Tri-tonX-100, 10% [v/v] glycerol, and 10 mg/L [*p*-amidinophenyl] methylsulfonyl fluoride). The luciferase activity and the alkaline phosphatase activity were assayed with Picagene (Toyo Ink, Tokyo, Japan) and CDP-Star (Roche) as substrates and measured by ARVO MX (Perkin Elmer, Waltham, MA, USA). The alkaline phosphatase assay was carried out in 98.4 mM glycine–NaOH (pH 10.5), 0.1 mM $ZnCl_2$, and 1 mM $MgCl_2$.

Phosphate-affinity SDS-PAGE. Phosphate-affinity SDS-PAGE was carried out with Phos-tag acrylamide and PVDF membranes (Millipore, Billierica, MA, USA). Briefly, 1×10^5 U2OS-GFP-TAZ cells were harvested with 100 μL of 1× Laemmli sample buffer. Then 400 μL methanol, 100 μL $CHCl_3$, and 300 μL distilled water were sequentially added. The mixture was centrifuged at 12 900 *g* for 5 min at room temperature. The supernatant was removed and the pellet was washed with 400 μL methanol. After centrifugation at

15 000 *g* for 5 min at room temperature, methanol was removed and evaporated. The pellet was resuspended in 60 μL 1× Laemmli sample buffer and analyzed on Phos-tag gel.

Large tumor suppressor kinase experiment. HEK293 cells (3×10^6) were plated in a 10-cm dish. Twenty-four hours later, the cells were transfected with pCIneoFLAG-LATS1 or pcDNA-LATS2-FLAG. Then, 24 h later, the cells were exposed to 10 μM IBS001594 or IBS015625 and cultured for another 24 h. The cells were harvested and the cell lysates were immunoblotted. The sequences around S909 of LATS1 and S871 of LATS2 and around T1079 of LATS1 and T1041 of LATS2 are identical and the phosphorylated LATS1 and LATS2 are detected with the same antibodies.

Co-immunoprecipitation and LUMIER assay. HEK293 cells were plated at 1×10^6 cells/well in a 6-well plate. Twelve hours later, the cells were transfected with various combinations of expression vectors. In order to adjust the total amount of DNA to 2.5 μg for all the points, pCIneoFH was added. Twenty-four hours later, the cells from each well were replated into three wells in a 12-well plate and treated with DMSO, 10 μM IBS001594 or IBS015625. The cells were harvested 24 h later and lysed in 500 μL lysis buffer (25 mM Tris-HCl [pH 7.4], 150 mM NaCl, 2 mM EDTA, 10 mM $MgCl_2$, 1% (v/v) TritonX-100, 10% (v/v) glycerol, 10 mg/L [*p*-amidinophenyl] methylsulfonyl fluoride, 10 mg/L leupeptin, and 2 mM DTT). The supernatant was collected after centrifugation at 20 000 *g* for 10 min. Fifty microliters of the supernatant was stocked as the input and 400 μL supernatant was used for the immunoprecipitation with anti-DYKDDDDK-tag beads. The immunoprecipitates were immunoblotted with the indicated antibodies. For the LUMIER assay, 50 μL Picagene (Toyo Ink) was added to the beads and the luciferase activity was measured by ARVO MX (Perkin Elmer). To confirm the efficiency of the immunoprecipitation, the beads were analyzed on SDS-PAGE and immunoblotted.

Soft agar and MTT assays. To indicate the dependency on TAZ and YAP1, H1299, OVCAR5, SW480, U2OS, U373, and U87MG cells were plated at 1×10^5/well in a 6-well plate and TAZ and YAP1 were knocked down. The cells were replated 48 h later at 2×10^4 cells/well in a 96-well plate for the MTT assay. The colorimetric assay was carried out with thiazolyl blue tetrazolium bromide (Sigma-Aldrich). The insoluble formazan was measured by SmartSpec 3000 (Bio-Rad, Hercules, CA, USA) at 570 nm. The cells were cultured for the indicated periods of time. To evaluate the effect of the compounds, the cells were cultured in the presence of DMSO or 10 μM each compound for 5 days. For the soft agar assay, 500 μL DMEM containing 10% (v/v) FBS, 0.5% (w/v) agarose, and 10 μM each compound was plated in one well of a 12-well plate. Then 500 μL DMEM containing 2500 U87MG cells, 10% (v/v) FBS, 0.3% (w/v) agarose, and 10 μM each compound was overlaid and kept for 1 h at room temperature. After that, 250 μL DMEM containing 10% (v/v) FBS was further overlaid and cultured for 3 weeks. The images were analyzed by ImageJ (http://imagej.nih.gov/ij/), and the area of cells were measured from three independent fields.

Statistical analysis. Two samples were compared with the Student's *t* test. Analysis of variance with Dunnett's test was used for the multiple comparison.

Results

Subcellular localization of GFP-TAZ in U2OS cells. We previously reported that the Hippo pathway is functional in U2OS cells and regulates the subcellular localization of GFP-YAP1.[18] We reasoned that the subcellular localization of GFP-TAZ is similarly regulated in U2OS cells by the Hippo pathway. As expected, GFP-TAZ was mainly distributed in the cytoplasm at high cell density, whereas it was accumulated in the nucleus at low cell density (Fig. 1a). We measured GFP signals in the nucleus and in the cytoplasm, calculated the ratio for 300 cells, and evaluated the distribution (Fig. 1a, histograms). This analysis confirmed that the cells with the high n/c ratio increase at the low density, while the cells with the low n/c ratio increase at the high density. Knockdown of LATS1/2 increased the cells with the high n/c ratio (Fig. 1b). Conversely, forskolin, which activates LATS1/2, increased the cells with the low n/c ratio (Fig. 1c). These findings support that the subcellular localization of GFP-TAZ is regulated by the Hippo pathway in U2OS cells.

Chemical compound library screening to search for compounds that decrease n/c ratio. We generated U2OS cells stably expressing GFP-TAZ (U2OS-GFP-TAZ cells) and applied 18 606 chemical compounds to these cells at the low cell density for 24 h. In the first screening, 104 compounds increased the n/c ratio (robust Z score > 3.0), whereas 86 compounds decreased it (robust Z score < −3.0) (Fig. 2a). As we aimed to find TAZ inhibitors, we focused on the latter 86 compounds. We viewed the cells treated with these compounds and excluded 32 compounds with remarkable cytotoxicity against U2OS cells or autofluorescence. We retested the remaining 54 compounds. We set the n/c ratio for the DMSO-treated control cells at 1.0 and calculated the relative n/c ratio for the cells treated with each compound. The mean of the n/c ratios of 54 compounds was 0.95 and 33 compounds decreased the n/c ratio to less than the mean value (Fig. 2b). The recruitment of GFP-TAZ from the nucleus to the cytoplasm was confirmed under the microscope (Fig. 2c). In the canonical Hippo pathway, the phosphorylation at serine 89 is the most important determinant of the cytoplasmic segregation of TAZ. To test whether or not the phosphorylation at serine 89 is required for the compounds to recruit GFP-TAZ to the cytoplasm, we expressed GFP-TAZ S89A in U2OS cells and treated the cells with 33 compounds. Of them, 32 compounds did not recruit GFP-TAZ S89A, showing that these compounds work on GFP-TAZ through the phosphorylation at serine 89 (Fig. 2d). One compound, IBS008420, shifted GFP-TAZ S89A from the nucleus to the cytoplasm. This finding suggests that IBS008420 regulates the subcellular localization of GFP-TAZ independently of the phosphorylation at serine 89.

Effect on TEAD-reporter assay. TAZ interacts with numerous transcription factors but TEAD proteins are the most important in the induction of the epithelial–mesenchymal transition in cancer cells.[28] We next examined whether TAZ inhibitor candidates inhibit the TEAD reporter activity in HEK293 cells. Six compounds (IBS000540, IBS008420, IBS001594, IBS011123, IBS015181, and IBS015625) decreased the activity by more than 20% (Fig. 3a, black columns). We found during the reporter assay that IBS011123 showed strong cytotoxicity against HEK293 cells. We omitted IBS011123 and decided to study the remaining five compounds (for simplicity, we designated these compounds TEAD reporter suppressors). Twenty-one compounds did not significantly affect the TEAD reporter activity in HEK293 cells (Fig. 3a, gray columns). Surprisingly, six compounds enhanced the TEAD reporter activity (Fig. 3a, white columns). We also carried out the reporter assay in U2OS cells. Even in these cells, not all compounds suppressed the reporter activity, but 14 compounds
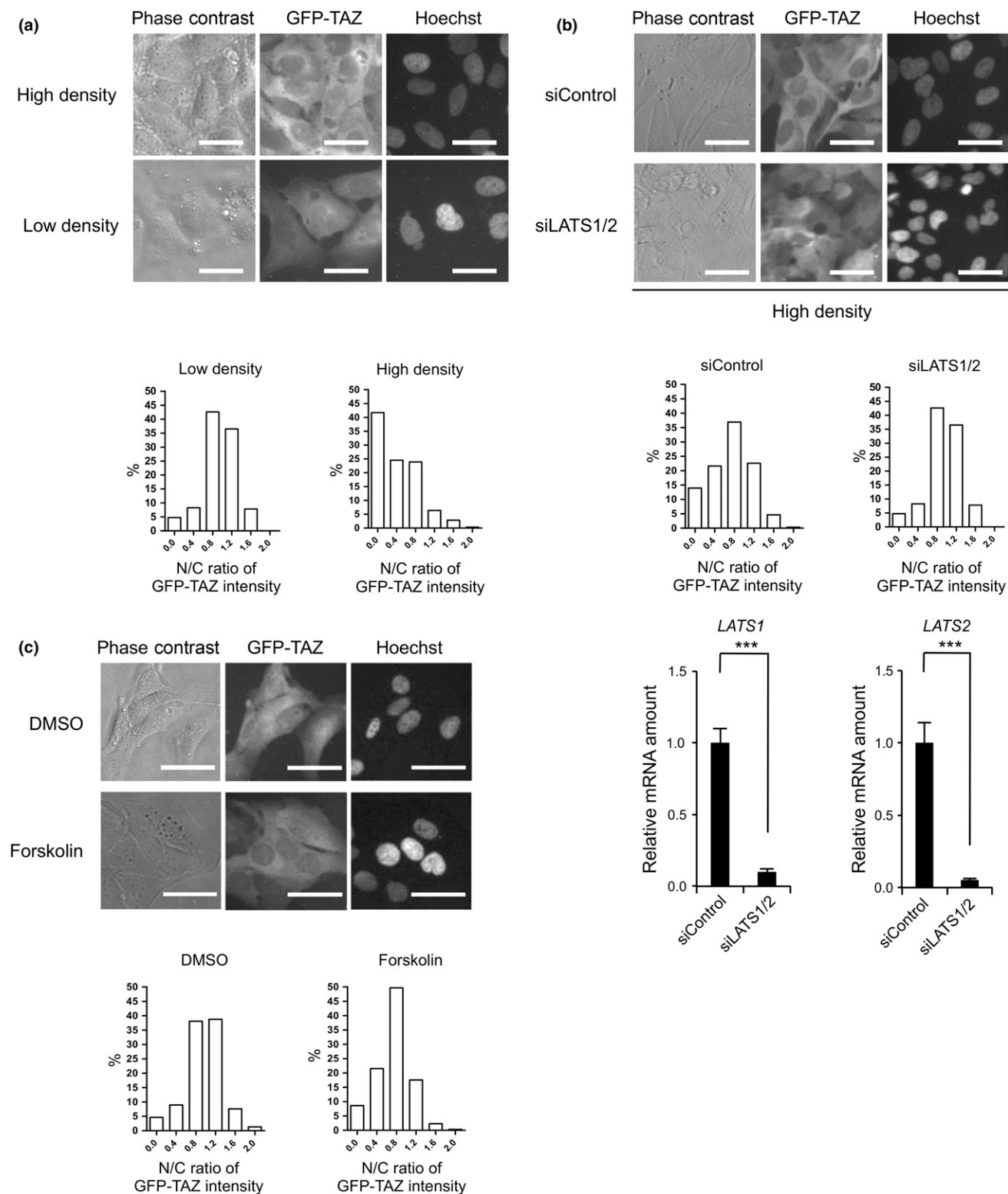
Fig. 1. Green fluorescent protein–transcriptional co-activator with PDZ-binding motif (GFP-TAZ) in human osteosarcoma U2OS cells. (a) U2OS cells expressing GFP-TAZ were plated at 9000 cells/well (high density) and 3000 cells/well (low density) in a 96-well plate. Sixteen hours later, the cells were fixed and the nuclei were visualized with Hoechst 33342. GFP signals inside and outside the nucleus were measured in 300 cells and the ratio of the nuclear GFP to the cytoplasmic GFP (N/C ratio) was calculated. The histograms show the distribution of the cells with the indicated n/c ratios. Bar = 50 μm. (b) U2OS-GFP-TAZ cells were plated at 1×10^6 cells/well in a 6-well plate and transfected with control dsRNA or dsRNAs against large tumor suppressor kinases (LATS)1/2. Cells were replated 48 h later at 9000 cells/well in a 96-well plate. GFP signals were evaluated 24 h later. The knockdown efficiency was tested for LATS1/2 mRNAs by quantitative RT-PCR (bottom histograms). (c) U2OS-GFP-TAZ cells were plated at 3000 cells/well in a 96-well plate. Twenty-four hours later, the cells were treated with DMSO or 10 μM forskolin, and cultured for another 24 h. LATS1/2 knockdown increased the cells with the high n/c ratios, but forskolin increased the cells with the low n/c ratios.
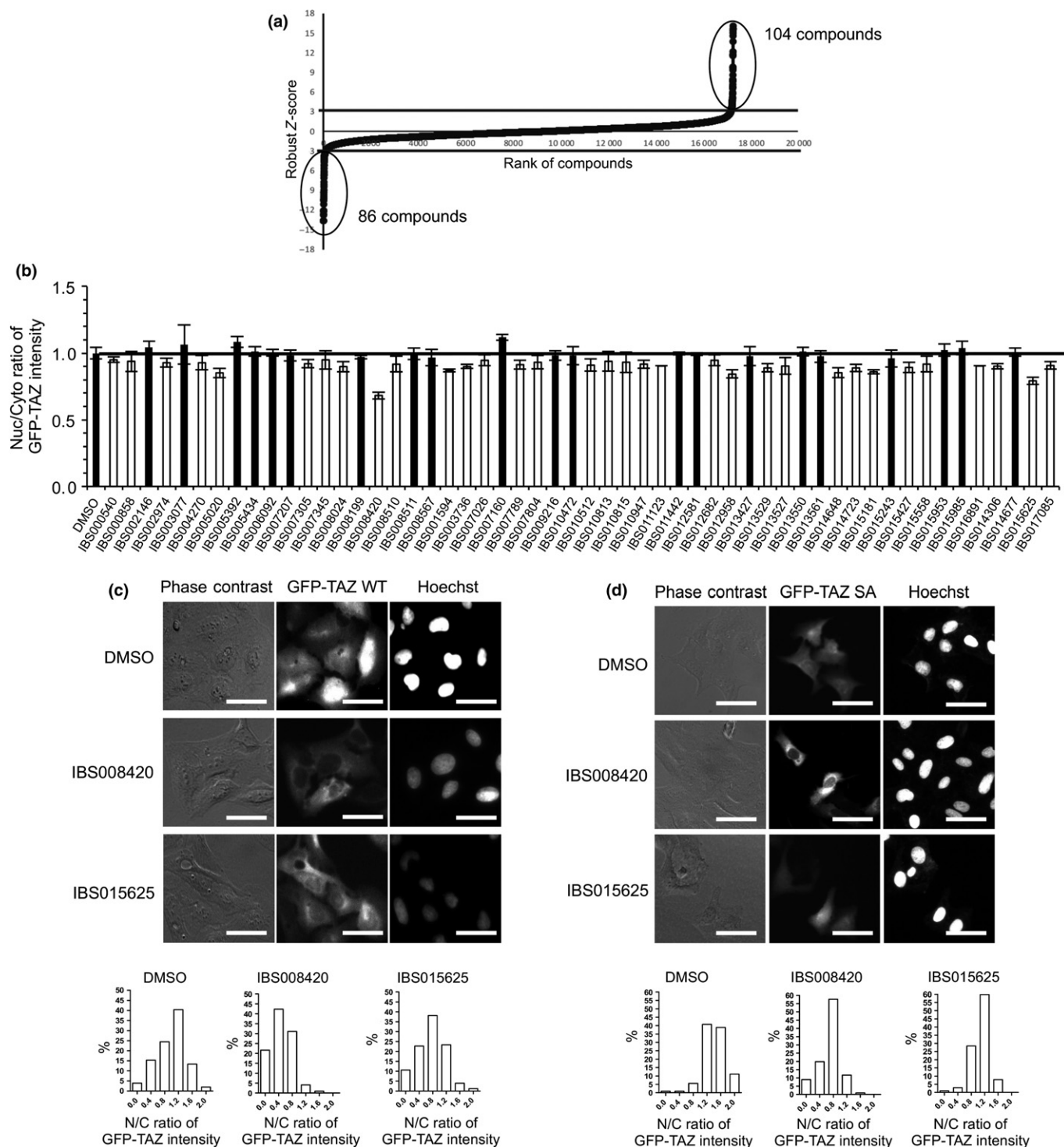
Fig. 2. Summary of chemical compound library screening for transcriptional co-activator with PDZ-binding motif (TAZ) inhibitors. (a) U2OS-GFP-TAZ cells were plated at 3000 cells/well in a 96-well plate. After 24 h, the compounds were applied to the cells at the concentration of 10 μM. The cells were fixed 24 h later and analyzed. Eighty compounds were tested in each plate and robust Z-scores were determined for each plate. Of 18 606 compounds, 104 increased the nucleus/cytoplasm (N/C) ratio (robust Z-score > 3), whereas 86 compounds decreased the n/c ratio (robust Z-score < −3). Horizontal bars indicate Z-scores of 3 and −3. (b) Cells treated with the 86 compounds were viewed under the microscope; 32 with remarkable cytotoxicity or autoimmunofluorescence were excluded. Fifty-four compounds were compared with control (DMSO). The mean of the n/c ratios of the DMSO-treated cells was set at 1.0 and the relative n/c ratio of the cells treated with each compound was calculated. The mean of the relative n/c ratios of 54 compounds was 0.95 (horizontal bar). Thirty-three compounds (white columns) decreased the n/c ratio less than the mean. (c, d) Representative images that show the effect of the compounds on the distribution of GFP-TAZ and GFP-TAZ S89A in U2OS-GFP-TAZ cells (c) and GFP-TAZ S89A transiently expressed in U2OS cells (d). Cells were treated with DMSO, 10 μM IBS008420, or 10 μM IBS015625 for 24 h. In (c), under the treatment of IBS008420 or IBS015625, the cells with lower n/c ratios increased. In (d), IBS008420 induces the recruitment of GFP-TAZ S89A into the cytoplasm and increases the cells with the lower n/c ratios, while IBS015625 does not.
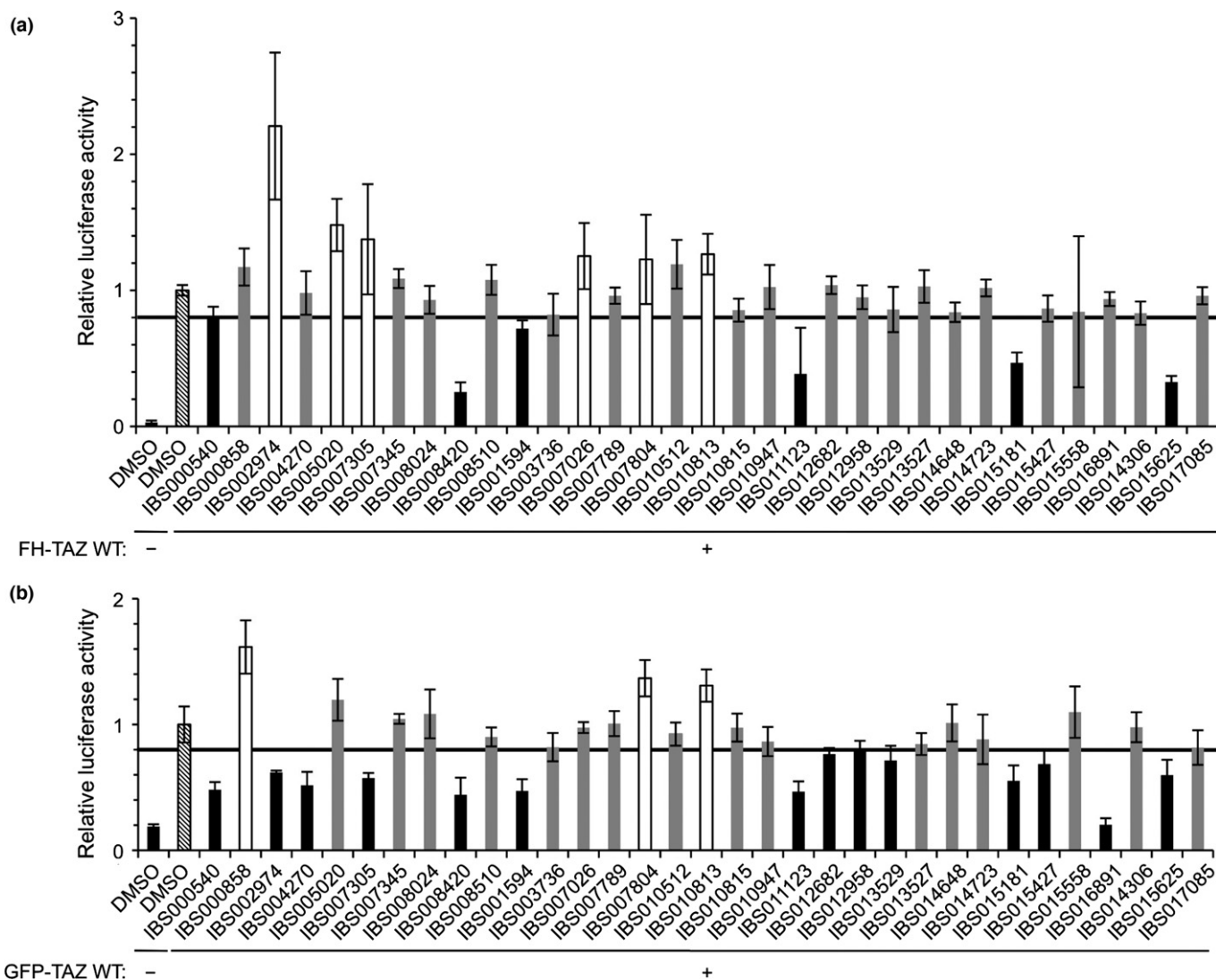
Fig. 3. Effect of 33 transcriptional co-activator with PDZ-binding motif (TAZ) inhibitor candidates on TEA domain reporter activity. HEK293 (a) and U2OS (b) cells were transfected with 8xGT-IIC-δ51 *Luc*II and pCIneoFH-TAZ except the first column, in which only the reporter was expressed, and treated with DMSO or 10 μM each compound for 18 h. Each compound was tested in triplicate. Data are shown as the mean with SD. TAZ co-expression increased the reporter activity (first and second columns). The mean value of the second column was set at 1.0. The bar indicates 0.8. (a) Six compounds reduced the reporter activity to <80% (black) and six enhanced the reporter activity (white). The remaining 21 compounds did not significantly affect the reporter activity (gray). (b) In U2OS cells, 14 (black) and 3 (white) compounds reduced and enhanced the reporter activity, respectively.

decreased it (Fig. 3b). Of note, six compounds that suppressed the reporter activity in HEK293 cells also reduced the reporter activity in U2OS cells. As we wanted to know whether the GFP-TAZ-based assay provides the compounds

that suppress cancer cells, we focused on five TEAD reporter suppressors.

Effect on phosphorylation of TAZ. With the concurrence of the TEAD reporter assay, we examined how the compounds

Fig. 4. Effect of 33 transcriptional co-activator with PDZ-binding motif (TAZ) inhibitor candidates on phosphorylation of TAZ. (a–c) U2OS-GFP-TAZ cells were plated at 1×10^5 cells/well in a 6-well plate and treated with 10 μM each compound for 24 h. Cell lysates were analyzed on Phos-tag gels and immunoblotted (IB) with anti-phoshpo-Ser89 antibody (upper blots) and anti-GFP antibody (lower blots). As H_2O_2 is known to activate MST kinases, the lysates of the cells treated with 1 mM H_2O_2 for 30 min were run as a positive control.[46] The lowest bands (arrows) were detected only with anti-GFP antibody and the upper bands (arrowheads) were detected with both anti-phospho-Ser89 and anti-GFP antibodies. The immunoblottings with anti-GFP and anti-β-actin antibodies in the conventional SDS-PAGE are shown at the bottom. (b) Signal intensities of the upper phosphorylated and the lowest unphosphorylated (un-P) TAZ were measured by imageJ and the ratio of the lowest signal over the total signals was calculated for each compound. Then the value for the DMSO-treated cells was set at 1.0 and the relative value for the cells treated with each compound was depicted as the histograms. The bold horizontal bar indicates the value 1.0. Among the five TEA domain (TEAD) reporter suppressors, IBS000540, IBS001594, and IBS015625 decreased unphosphorylated TAZ (white stars). IBS008420 and IBS015181 increased unphosphorylated TAZ (black asterisks). (a) IBS008420 remarkably increased unphosphorylated TAZ (white arrowhead). (c) Effect of IBS000540, IBS001594, and IBS015625 on TEAD reporter activity in the presence of Yes-associated protein 1 (YAP1). The reporter assay was carried out using pFLAG-YAP1. All three compounds suppressed YAP1-dependent TEAD reporter activity. (d) Structures of IBS000540, IBS001594, and IBS015625.
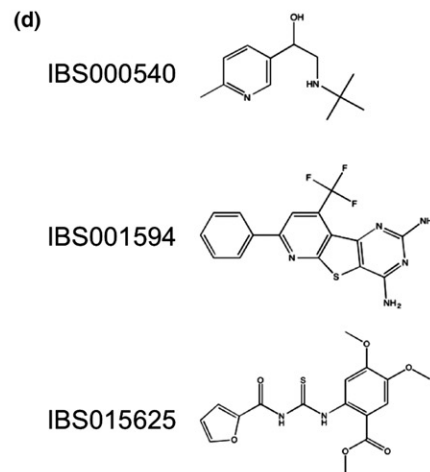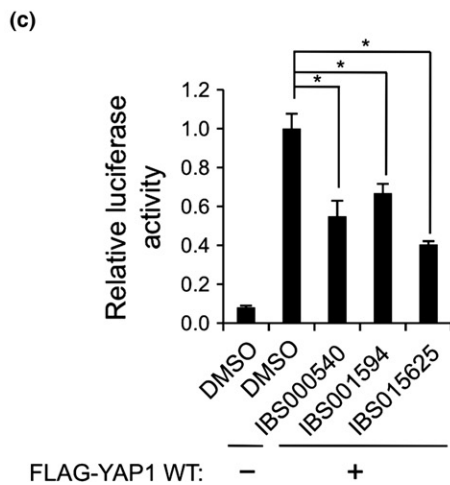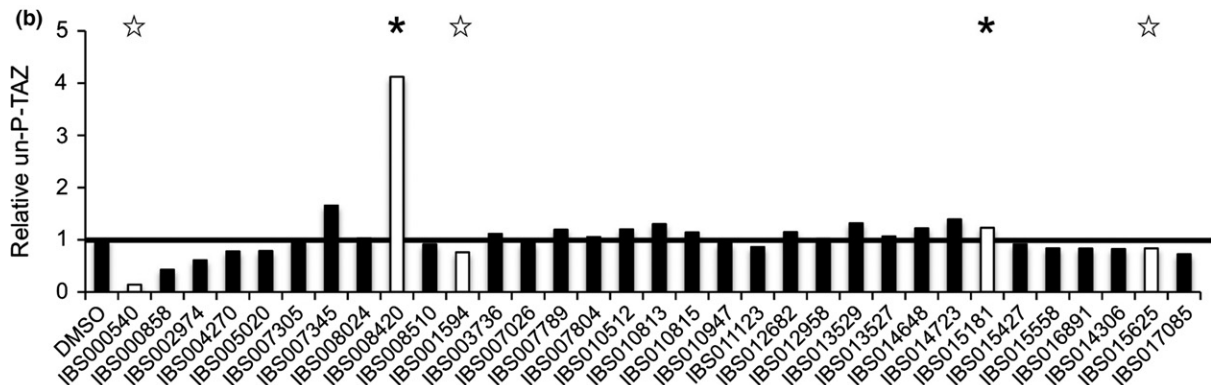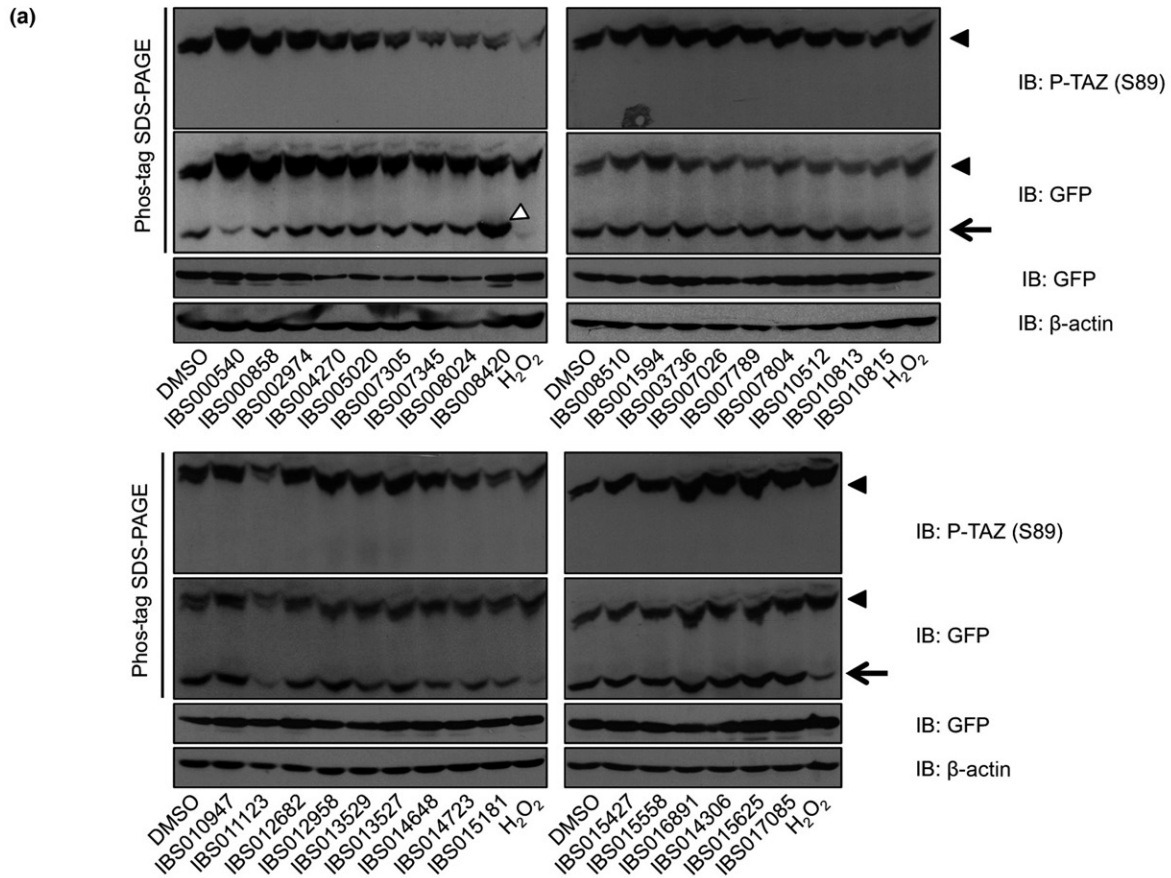
affect the phosphorylation of TAZ. According to the canonical Hippo pathway, the compounds that decrease the n/c ratio of GFP-TAZ are predicted to increase the phosphorylated TAZ and decrease the unphosphorylated TAZ. We treated U2OS-GFP-TAZ cells with the compounds for 24 h and analyzed the cell lysates by use of Phos-tag SDS-PAGE and immunoblotting. The lowest bands were detected with anti-GFP antibody but not with anti-phospho-S89 TAZ antibody (Fig. 4a, black arrows). The upper bands were detected with both antibodies and thought to correspond to the phosphorylated TAZ (Fig. 4a, black arrowheads). We measured the signals of upper and lower bands in the Phos-tag gels and calculated the relative intensity of the signal of the lower band for each compound. Contrary to our prediction, not all the compounds decreased the relative amount of unphosphorylated TAZ (Fig. 4b). We also evaluated the total TAZ by immunoblotting with anti-GFP antibody in the conventional SDS-PAGE. The total TAZ was largely unchanged, but decreased in the cells treated with certain compounds. We speculated that phosphorylated TAZ might be rapidly degraded, which made it difficult to observe the relative decrease of unphosphorylated TAZ. Notably, among five TEAD reporter suppressors that we focused on in this study, IBS000540, IBS001594, and IBS015625 decreased unphosphorylated TAZ (Fig, 4b, white stars). However, IBS008420 remarkably increased it and IBS015181 also slightly increased it (Fig. 4a, white arrowhead; Fig. 4b, black asterisks). These findings imply that IBS000540, IBS001594, and IBS015625 inhibit TAZ through the canonical Hippo pathway. These compounds inhibited TEAD reporter activity in the presence of YAP1 as well as TAZ, suggesting that these compounds work through the regulatory mechanism shared by YAP1 and TAZ and further corroborating that their targets reside in the canonical Hippo pathway (Fig. 4c). In contrast, IBS008420 may suppress TAZ through an unidentified mechanism. In this study, we analyzed IBS000540, IBS001594, and IBS015625 (Fig. 4d).

Effect of IBS000540, IBS001594, and IBS015625 on cancer cells. As we wanted to know whether screening by the use of U2OS-GFP-TAZ cells allows us to identify the compounds that inhibit TAZ and suppress cancer cells, we next examined the effect of IBS000540, IBS001594, and IBS015625 on cancer cells. We first knocked down TAZ and YAP1 in human lung cancer H1299, ovarian cancer OVCAR5, colon cancer SW480, osteosarcoma U2OS, glioblastoma U373, and glioblastoma U87MG cells (Fig. 5a). The MTT assay indicated that the knockdown of TAZ and YAP1 compromised the viability of all of these cells (Fig. 5a). This finding means that a compound that inhibits TAZ and YAP1 should suppress the viability of these cells. We applied IBS000540, IBS001594, and IBS015625 to each cell line. Although IBS000540 did not show any significant effect, IBS001594 reduced the cell viability of all the tested cell lines except H1299 (Fig. 5b).

IBS0015625 was effective for OVCAR5 and U87MG cells (Fig. 5b). IBS001594 and IBS015625 suppressed the colony formation of U87MG cells in the soft agar (Fig. 5c). mRNAs of *CTGF* and *Cyr61*, the target genes of TEAD, were decreased in U87MG cells treated with IBS001594 and IBS015625 (Fig. 5d).
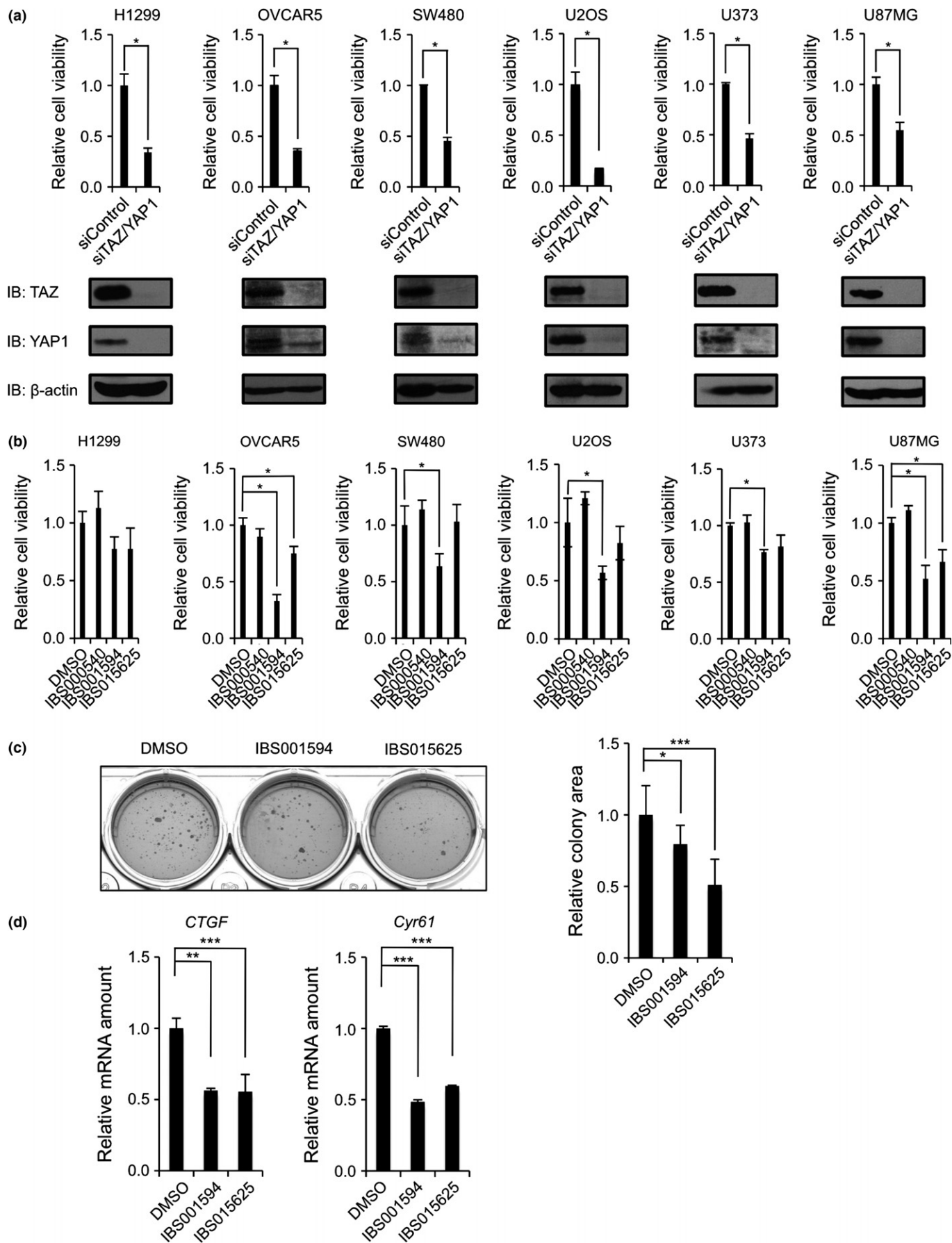
Effect of IBS001594 and IBS015625 on LATS1/2 activity and TAZ–LATS1/2 interaction. We next asked how IBS001594 and IBS015625 decrease the unphosphorylated TAZ. To confirm that these compounds increase the phosphorylated TAZ through LATS1/2, we knocked down LATS1/2. IBS001594 and IBS015625 did not increase the phosphorylated TAZ in LATS1/2-depeleted cells (Fig. 6a). We next tested whether the compounds activate LATS1/2. When LATS1/2 are activated, Ser909/Ser871 and Thr1079/Thr1041 are phosphorylated and LATS1/2 activities can be estimated based on the phosphorylation at these sites.[29] We expressed FLAG-LATS1/2 in HEK293 cells, treated the cells with the compounds, immunoprecipitated FLAG-LATS1/2, and immunoblotted them with the antibodies against phosphorylated Ser909/Ser871 and Thr1079/Thr1041. IBS001594 enhanced phosphorylation at Ser909 and Thr1079 of LATS1, but IBS015625 suppressed phosphorylation (Fig. 6b, left panel). Likewise, IBS001594 increased the phosphorylation of LATS2 but IBS015625 decreased it (Fig. 6b, right panel). We expressed GFP-TAZ with FLAG-LATS1/2 in HEK293 cells and carried out co-immunoprecipitation. This experiment revealed that neither IBS001594 nor IBS015625 affected the interaction between TAZ with LATS1/2 (Fig. 6c).

Effect of IBS001594 and IBS015625 on interaction between TAZ and protein phosphatases. The phosphorylation of TAZ is also regulated by protein phosphatases (PP).[30] We expressed luciferase-fused TAZ with FLAG-PP1A and FLAG-PP2A in HEK293 cells, treated the cells with the compounds, immunoprecipitated FLAG-PP1A and FLAG-PP2A, and measured the luciferase activity in the immunoprecipitates. IBS001594 augmented the co-immunoprecipitation of TAZ with PP1A and PP2A, but IBS015625 had no effect (Fig. 7). These findings suggest that IBS001594 activates LATS kinases and enhances the interaction of TAZ with phosphatases and that the balance shifts to the increase of the phosphorylation. How IBS015625 decreases the unphosphorylated TAZ is not clear, but we can surmise that IBS001594 and IBS015625 have distinct molecular targets.

Discussion

The co-transcriptional activators, TAZ and YAP1, attract attention as the two-faced drug targets in medicine.[31] Both are negatively regulated by the tumor-suppressive Hippo pathway.[1,2] In cancers, the deregulation of the Hippo pathway and gene amplification enhance the activity of TAZ and

Fig. 5. Effect of IBS000540, IBS001594, and IBS015625 on cancer cells. (a) H1299, OVCAR5, SW480, U2OS, U373, and U87MG cells (1.5×10^5) were cultured in a 6-well plate and transfected with control dsRNA or the mixture of transcriptional co-activator with PDZ-binding motif (TAZ)-targeted and Yes-associated protein 1 (YAP1)-targeted dsRNAs. The cells were replated at 1×10^3 cells/well in a 96-well plate and cultured for 96 h. The colorimetric assay was carried out with thiazolyl blue tetrazolium bromide. Insoluble formazan was measured by SmartSpec 3000 (Bio-Rad) at 570 nm. Immunoblottings (IB) of TAZ and YAP1 are shown at the bottom. Data are the mean ± SD. *$P < 0.05$. (b) Cells were plated at 1×10^3 cells/well in a 96-well plate and cultured with DMSO or 10 μM each compound. MTT assay was carried out 5 days later. Data are the mean ± SD. *$P < 0.05$. At a glance, IBS001594 and IBS015625 suppress H1299 growth, but the effect is not statistically significant. (c) Soft agar assay was carried out and the colony formation was evaluated. IBS001594 and IBS015625 suppressed the colony formation of U87MG in soft agar. Data are the mean ± SD. *$P < 0.05$; ***$P < 0.001$. (d) U87MG cells were plated at 2×10^5 cells/well in a 6-well plate. After 24 h, each compound was added to a final concentration of 10 μM. Total RNA was extracted 48 h later and quantitative RT-PCR was carried out. IBS001594 and IBS015625 suppressed the expression of *CTGF* and *Cyr61*. **$P < 0.01$; ***$P < 0.001$.
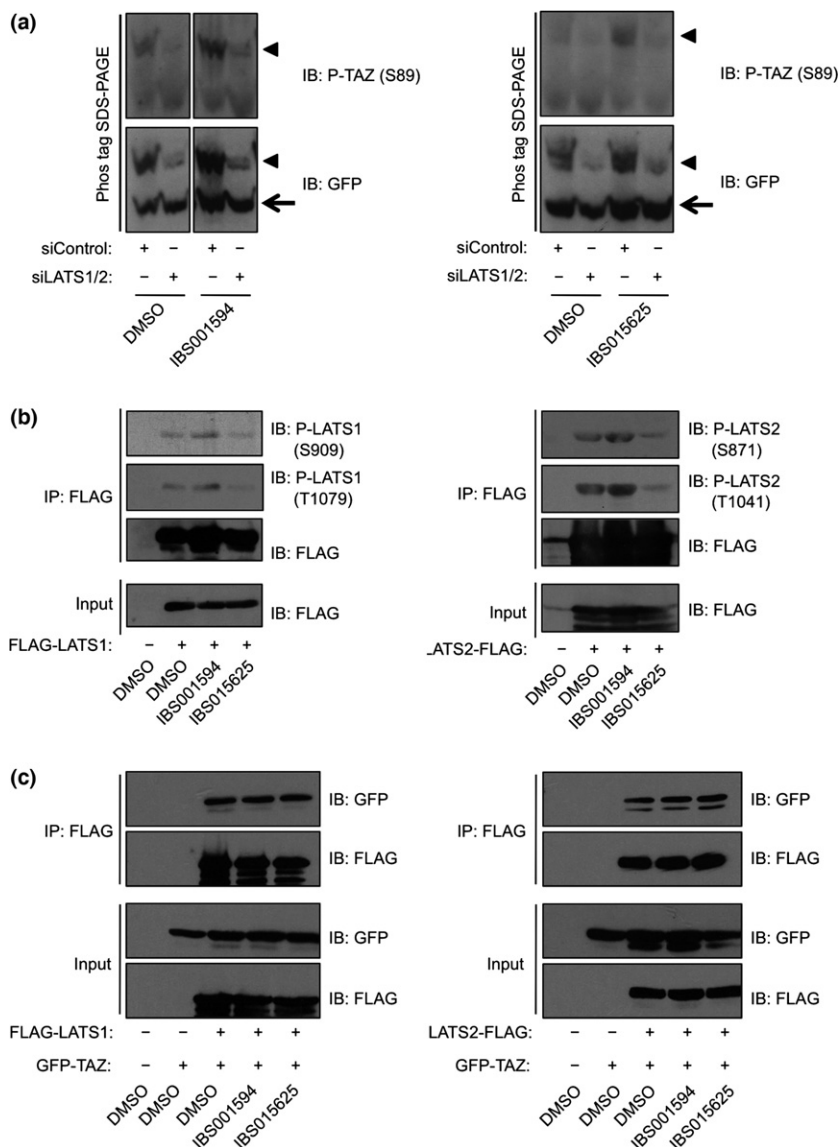
Fig. 6. Effect of IBS001594 and IBS015625 on activity of large tumor suppressor kinases (LATS1/2) and interaction between transcriptional co-activator with PDZ-binding motif (TAZ) and LATS1/2. (a) U2OS-GFP-TAZ cells were plated at 1.5×10^5 cells/well in a 6-well plate and transfected with control dsRNA or combined dsRNAs against LATS1/2. Cells were replated 48 h later at 1×10^5 cells/well in a 6-well plate. Cells were treated 24 h later with DMSO, 10 μM IBS001594, or 10 μM IBS015625 for 24 h. Cell lysates were analyzed on Phos-tag gels and immunoblotted (IB) with anti-phospho-Ser89 TAZ and anti-GFP antibodies. IBS001594 and IBS015625 increased phosphorylated TAZ in control cells, but not in LATS1/2-depleted cells. (b) HEK293 cells (3×10^6) were plated in a 10-cm dish and transfected 24 h later with pCIneoFLAG-LATS1 (15 μg). To express FLAG-tagged LATS2, HEK293 cells were plated at 8×10^5 cells/well in a 6-well plate and transfected with pcDNA-LATS2-FLAG (2 μg). After 24 h of transfection, the cells were treated with DMSO, 10 μM IBS001594, or 10 μM IBS015625 and further cultured for 24 h. Immunoprecipitation (IP) was carried out with anti-DYKDDDDK-tag beads. The inputs and immunoprecipitates were immunoblotted with anti-S909/S871 LATS1/2, anti-T1079/T1041 LATS1/2, and anti-FLAG antibodies. (c) HEK293 cells were plated 3×10^6 cells/10-cm dish for LATS1 or at 8×10^5 cells/well in a 6-well plate for LATS2. Cells were transfected 24 h later with the indicated combination of pCIneoFLAG-LATS1 (15 μg), pcDNA-LATS2-FLAG (1 μg), pCIneoGFP-TAZ (1 μg), or pCIneoFH (1 μg). Cells were treated with DMSO, 10 μM IBS001594, or 10 μM IBS015625. Immunoprecipitation (IP) was carried out with anti-DYKDDDDK-tag beads. The inputs and immunoprecipitates were immunoblotted with indicated antibodies.

YAP1.[7,32,33] The high activation of TAZ or YAP1 confers malignant properties to cancer cells and results in metastasis and drug resistance. The suppression of TAZ and YAP1 is important to control cancers and may improve the clinical prognosis. TAZ and YAP1 play important roles in adult tissue stem cells.[34,35] YAP1 activity is essential for tissue repair in intestine, liver, and skin,[36–39] and YAP1 activation protects heart after cardiac infarction.[40,41] TAZ is also required for skin repair and promotes osteogenesis in mesenchymal stem cells and myogenesis in myoblasts.[42,43] Thus, screening for the inhibitors and activators of TAZ and YAP1 is one of the central issues in current drug discovery. The main regulators of TAZ and YAP1 are LATS kinases and protein phosphatases. The phosphorylation by LATS kinases induces the translocation of TAZ and YAP1 from the nucleus to the cytoplasm, and triggers degradation. In contrast, unphosphorylated TAZ and YAP1 regulate gene transcription in the nucleus. Thereby, the subcellular localization of TAZ and YAP1 reflects the activity of TAZ and YAP1. We used the localization of GFP-YAP1 in U2OS cells as the read-out and revealed that dobutamine inhibits YAP1 through β-adrenergic receptor.[18] Sorrentino et al. determined the subcellular localization

of endogenous TAZ and YAP1 in MDA-MB-231 cells and showed that statin inhibits TAZ and YAP1.[44] Jang et al. expressed GFP-TAZ in COS-7 cells and identified novel TAZ activators.[45] In this study, we expressed GFP-TAZ in U2OS cells and applied small chemical compounds to these cells. We aimed in this study to validate that this cell-based assay provides the compounds that inhibit TAZ through the Hippo pathway.

Green fluorescent protein–TAZ is accumulated in the cytoplasm in U2OS cells at high cell density and in the nucleus at low cell density (Fig. 1a). The depletion of LATS kinases reduced the cytoplasmic accumulation of GFP-TAZ at low cell density, whereas forskolin, the activator of LATS kinases, increased the cytoplasmic accumulation (Fig. 1b,c). These findings support that the Hippo pathway regulates the localization of GFP-TAZ in U2OS cells. We applied 18 606 chemical compounds to these cells, and obtained 33 compounds that induced the cytoplasmic shift of GFP-TAZ (Fig. 2). Of them, 32 compounds failed to recruit GFP-TAZ S89A. These 32 compounds are thought to induce the cytoplasmic translocation of GFP-TAZ through phosphorylation at Ser89, which is the most important molecular determinant of the regulation by the

Fig. 7. Effect of IBS001594 and IBS015625 on interaction between transcriptional co-activator with PDZ-binding motif (TAZ) and protein phosphatases (PP). HEK293 cells were transfected with the indicated combination of pCIneoFHF-PP1A (1 μg), pCIneoFHF-PP2A (1 μg), pCIneoLuc-TAZ (1 μg), or pCIneoGFP (1 μg). Cells were treated with DMSO, 10 μM IBS001594, or 10 μM IBS015625 for 24 h. Immunoprecipitation (IP) was carried out with anti-DYKDDDDK-tag beads and luciferase activities in the immunoprecipitates were measured. The first column represents the basal amount of luciferase that attached to FLAG-agarose beads. The mean value of the immunoprecipitates from the DMSO-treated cells was set as 1.0. Immunoprecipitates were immunoblotted (IB) with anti-FLAG antibody to show that FLAG-PP1A or FLAG-PP2A was equally immunoprecipitated (columns 2–4). Lower histograms show that the total luciferase activities in the input were almost the same for all points. *$P < 0.05$. ns, not significant.
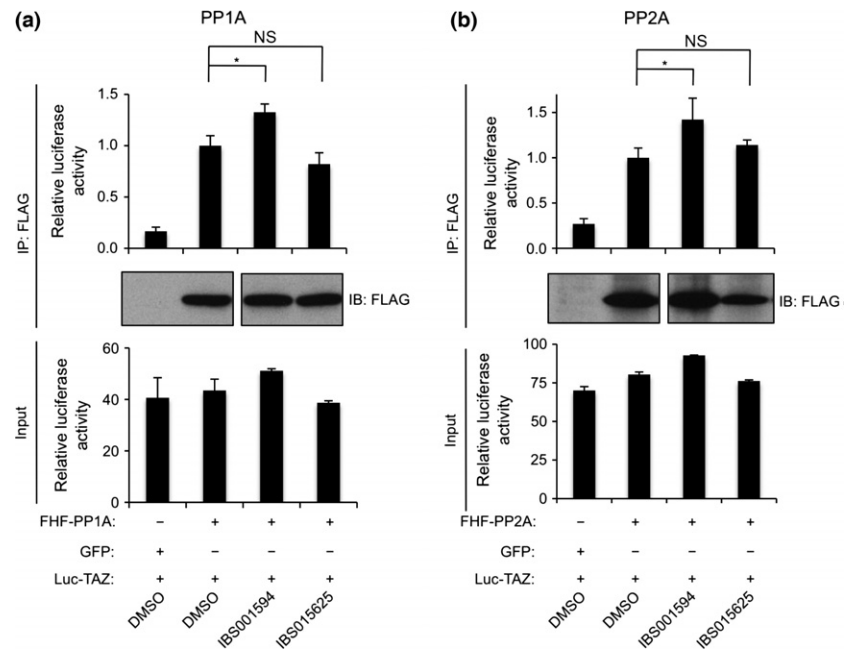
canonical Hippo pathway. Unexpectedly, only 6 and 14 compounds significantly suppressed the TEAD reporter activity in HEK293 and U2OS cells, respectively (Fig. 3). Most compounds did not show any significant effect, and certain compounds enhanced the TEAD reporter activity. We used the n/c ratio as the read-out in the first screening. A compound that increases both cytoplasmic and nuclear TAZ can be obtained if the increase in the cytoplasm is larger than that in the nucleus and such a compound fails to suppress the reporter activity. Eight compounds suppressed reporter activity in U2OS cells, but not in HEK293 cells. In U2OS cells, the subcellular localization of GFP-TAZ is regulated in a cell density-dependent manner, supporting that the Hippo pathway is intact. In contrast, the Hippo pathway may be deregulated in HEK293 cells. We speculate that the targets of these compounds are missing in HEK293 cells.

As discussed above, 32 compounds apparently require the phosphorylation at Ser89 to inhibit TAZ. However, in the Phos-tag gel analysis, the increase of phosphorylated TAZ was not clearly detected for all compounds (Fig. 4). We suspect that swift degradation may obscure the increase of phosphorylated TAZ. Among five compounds that significantly suppress TEAD reporter activity, IBS008420 and IBS015181 did not increase phosphorylated TAZ. On the contrary, IBS008420 remarkably increased unphosphorylated TAZ. This finding is consistent with the fact that IBS008420 recruits TAZ S89A to the cytoplasm. IBS008420 is thought to modulate TAZ through an unknown mechanism that is independent of the phosphorylation of TAZ. In the IBS015181-treated cells, the signals of both phosphorylated and unphosphorylated TAZ were reduced. We speculate that IBS015181 increases phosphorylated TAZ, causes its quick degradation, and fails to show the relative increase of phosphorylated TAZ. To understand how IBS008420 and IBS015181 inhibit TAZ, we are now trying to identify their targets. IBS000540, IBS001594, and IBS015625 decreased unphosphorylated TAZ. As these three compounds suppress YAP1-dependent TEAD reporter activity, their targets are likely to reside in the regulatory machinery shared by TAZ and YAP1 (Fig. 4c). However, IBS001594 activates LATS

kinases and strengthens the interaction of TAZ with protein phosphatases; IBS015625 rather weakens the activity of LATS kinases and has no effect on the interaction of TAZ with protein phosphatase (Figs. 5–7). These findings indicate that this cell-based assay gives various compounds with distinct molecular targets.

As IBS000540, IBS001594, and IBS015625 decreased the unphosphorylated TAZ and suppressed TAZ-dependent TEAD reporter activity, we expected that these compounds suppress the proliferation of cancer cells. Indeed, IBS001594 suppressed various cancer cells (Fig. 5). IBS015625 also inhibited cell proliferation in certain cancer cells. However, IBS000540, which strongly increases phosphorylated TAZ, does not show a significant effect on cancer cells (Fig. 5). Namely, not all the compounds that increase phosphorylated TAZ and recruit TAZ to the cytoplasm are effective to control cancer cells. In the phosphorylation experiment, the cells were treated with IBS000540 for 24 h, but in the MTT assay, the cells were cultured for 72 h. Although we have not examined how long the IBS000540-mediated increase of phosphorylated TAZ is maintained, we suspect that the effect of IBS000540 may be short-lived. This observation reminds us of the fact that dobutamine, although it increases the phosphorylation of YAP1 and inhibits YAP1-dependent TEAD reporter activity, did not show significant effects on cancer cells in our experiments.

In conclusion, the cell-based assay using U2OS cells expressing GFP-TAZ provides the compounds that inhibit TAZ through the Hippo pathway. However, the molecular targets and the effects on cancer cells differ. We can use this assay in the first screening for TAZ inhibitors and get an insight into the regulation of TAZ through the target identification. However, to obtain the compounds that can be developed into anticancer drugs, we need a second assay for further selection.

Disclosure Statement

References

1 Hong W, Guan KL. The YAP and TAZ transcription co-activators: key downstream effectors of the mammalian Hippo pathway. *Semin Cell Dev Biol* 2012; **23**: 785–93.
2 Kodaka M, Hata Y. The mammalian Hippo pathway: regulation and function of YAP1 and TAZ. *Cell Mol Life Sci* 2015; **72**: 285–306.
3 Kanai F, Marignani PA, Sarbassova D *et al*. TAZ: a novel transcriptional co-activator regulated by interactions with 14-3-3 and PDZ domain proteins. *EMBO J* 2000; **19**: 6778–91.
4 Lei QY, Zhang H, Zhao B *et al*. TAZ promotes cell proliferation and epithelial-mesenchymal transition and is inhibited by the hippo pathway. *Mol Cell Biol* 2008; **28**: 2426–36.
5 Liu CY, Zha ZY, Zhou X *et al*. The hippo tumor pathway promotes TAZ degradation by phosphorylating a phosphodegron and recruiting the SCF {beta}-TrCP E3 ligase. *J Biol Chem* 2010; **285**: 37159–69.
6 Huang W, Lv X, Liu C *et al*. The N-terminal phosphodegron targets TAZ/WWTR1 protein for SCFβ-TrCP-dependent degradation in response to phosphatidylinositol 3-kinase inhibition. *J Biol Chem* 2012; **287**: 26245–53.
7 Pan D. The hippo signaling pathway in development and cancer. *Dev Cell* 2010; **19**: 491–505.
8 Cordenonsi M, Zanconato F, Azzolin L *et al*. The Hippo transducer TAZ confers cancer stem cell-related traits on breast cancer cells. *Cell* 2011; **147**: 759–72.
9 Varelas X, Miller BW, Sopko R *et al*. The Hippo pathway regulates Wnt/beta-catenin signaling. *Dev Cell* 2010; **18**: 579–91.
10 Imajo M, Miyatake K, Iimura A, Miyamoto A, Nishida E. A molecular mechanism that links Hippo signalling to the inhibition of Wnt/β-catenin signalling. *EMBO J* 2012; **31**: 1109–22.
11 Azzolin L, Panciera T, Soligo S *et al*. YAP/TAZ incorporation in the β-catenin destruction complex orchestrates the Wnt response. *Cell* 2014; **158**: 157–70.
12 Zhou Z, Hao Y, Liu N, Raptis L, Tsao MS, Yang X. TAZ is a novel oncogene in non-small cell lung cancer. *Oncogene* 2011; **30**: 2181–6.
13 Yuen HF, McCrudden CM, Huang YH *et al*. TAZ expression as a prognostic indicator in colorectal cancer. *PLoS ONE* 2013; **8**: e54211.
14 Zhao B, Ye X, Yu J *et al*. TEAD mediates YAP-dependent gene induction and growth control. *Genes Dev* 2008; **22**: 1962–71.
15 Steinhardt AA, Gayyed MF, Klein AP *et al*. Expression of Yes-associated protein in common solid tumors. *Hum Pathol* 2008; **39**: 1582–9.
16 Xu MZ, Yao TJ, Lee NP *et al*. Yes-associated protein is an independent prognostic marker in hepatocellular carcinoma. *Cancer* 2009; **115**: 4576–85.
17 Hall CA, Wang R, Miao J *et al*. Hippo pathway effector Yap is an ovarian cancer oncogene. *Cancer Res* 2010; **70**: 8517–25.
18 Bao Y, Nakagawa K, Yang Z *et al*. A cell-based assay to screen stimulators of the Hippo pathway reveals the inhibitory effect of dobutamine on the YAP-dependent gene transcription. *J Biochem* 2011; **150**: 199–208.
19 Fujii M. Exploration of a new drug that targets YAP. *J Biochem* 2012; **152**: 209–11.
20 Zheng HX, Wu LN, Xiao H, Du Q, Liang JF. Inhibitory effects of dobutamine on human gastric adenocarcinoma. *World J Gastroenterol* 2014; **20**: 17092–9.
21 Ikeda M, Hirabayashi S, Fujiwara N *et al*. Ras-association domain family protein 6 induces apoptosis via both caspase-dependent and caspase-independent pathways. *Exp Cell Res* 2007; **313**: 1484–95.
22 Hirao K, Hata Y, Ide N *et al*. A novel multiple PDZ domain-containing molecule interacting with N-methyl-D-aspartate receptors and neuronal cell adhesion proteins. *J Biol Chem* 1998; **273**: 21105–10.
23 Yang Z, Nakagawa K, Sarkar A *et al*. Screening with a novel cell-based assay for TAZ activators identifies a compound that enhances myogenesis in

24 Kawano S, Maruyama J, Nagashima S *et al*. A cell-based screening for TAZ activators identifies ethacridine, a widely used antiseptic and abortifacient, as a compound that promotes dephosphorylation of TAZ and inhibits adipogenesis in C3H10T1/2 cells. *J Biochem* 2015; **158**: 413–23.
25 Ota M, Sasaki H. Mammalian Tead proteins regulate cell proliferation and contact inhibition as transcriptional mediators of Hippo signaling. *Development* 2008; **135**: 4059–69.
26 Abe Y, Ohsugi M, Haraguchi K, Fujimoto J, Yamamoto T. LATS2-Ajuba complex regulates gamma-tubulin recruitment to centrosomes and spindle organization during mitosis. *FEBS Lett* 2006; **580**: 782–8.
27 Bao Y, Sumita K, Kudo T *et al*. Roles of mammalian sterile 20-like kinase 2-dependent phosphorylations of Mps one binder 1B in the activation of nuclear Dbf2-related kinases. *Genes Cells* 2009; **14**: 1369–81.
28 Zhang H, Liu CY, Zha ZY *et al*. TEAD transcription factors mediate the function of TAZ in cell growth and epithelial-mesenchymal transition. *J Biol Chem* 2009; **284**: 13355–62.
29 Hergovich A. Regulation and functions of mammalian LATS/NDR kinases: looking beyond canonical Hippo signalling. *Cell Biosci* 2013; **3**: 32.
30 Liu CY, Lv X, Li T *et al*. PP1 cooperates with ASPP2 to dephosphorylate and activate TAZ. *J Biol Chem* 2011; **286**: 5558–66.
31 Johnson R, Halder G. The two faces of Hippo: targeting the Hippo pathway for regenerative medicine and cancer treatment. *Nat Rev Drug Discov* 2014; **13**: 63–79.
32 Harvey KF, Zhang X, Thomas DM. The Hippo pathway and human cancer. *Nat Rev Cancer* 2013; **13**: 246–57.
33 Nishio M, Otsubo K, Maehama T, Mimori K, Suzuki A. Capturing the mammalian Hippo: elucidating its role in cancer. *Cancer Sci* 2013; **104**: 1271–7.
34 Hiemer SE, Varelas X. Stem cell regulation by the Hippo pathway. *Biochim Biophys Acta* 2013; **1830**: 2323–34.
35 Mo JS, Park HW, Guan KL. The Hippo signaling pathway in stem cell biology and cancer. *EMBO Rep* 2014; **15**: 642–56.
36 Cai J, Zhang N, Zheng Y, de Wilde RF, Maitra A, Pan D. The Hippo signaling pathway restricts the oncogenic potential of an intestinal regeneration program. *Genes Dev* 2010; **24**: 2383–8.
37 Grijalva J, Huizenga M, Mueller K *et al*. Dynamic alterations in Hippo signaling pathway and YAP activation during liver regeneration. *Am J Physiol Gastrointest Liver Physiol* 2014; **307**: G196–204.
38 Yimlamai D, Christodoulou C, Galli GG *et al*. Hippo pathway activity influences liver cell fate. *Cell* 2014; **157**: 1324–38.
39 Lee MJ, Ran Byun M, Furutani-Seiki M, Hong JH, Jung HS. YAP and TAZ regulate skin wound healing. *J Invest Dermatol* 2014; **134**: 518–25.
40 Xin M, Kim Y, Sutherland LB *et al*. Hippo pathway effector Yap promotes cardiac regeneration. *Proc Natl Acad Sci USA* 2013; **110**: 13839–44.
41 Lin Z, von Gise A, Zhou P *et al*. Cardiac-specific YAP activation improves cardiac function and survival in an experimental murine myocardial infarction model. *Circ Res* 2014; **115**: 354–63.
42 Hong JH, Hwang ES, McManus MT *et al*. TAZ, a transcriptional modulator of mesenchymal stem cell differentiation. *Science* 2005; **309**: 1074–8.
43 Jeong H, Bae S, An SY *et al*. TAZ as a novel enhancer of MyoD-mediated myogenic differentiation. *FASEB J* 2010; **24**: 3310–20.
44 Sorrentino G, Ruggeri N, Specchia V *et al*. Metabolic control of YAP and TAZ by the mevalonate pathway. *Nat Cell Biol* 2014; **16**: 357–66.
45 Jang EJ, Jeong H, Kang JO *et al*. TM-25659 enhances osteogenic differentiation and suppresses adipogenic differentiation by modulating the transcriptional co-activator TAZ. *Br J Pharmacol* 2012; **165**: 1584–94.
46 Praskova M, Xia F, Avruch J. MOBKL1A/MOBKL1B phosphorylation by MST1 and MST2 inhibits cell proliferation. *Curr Biol* 2008; **18**: 311–21.

C2C12 cells and facilitates muscle repair in the muscle injury model. *Mol Cell Biol* 2014; **34**: 1607–21.